JOURNAL OF ACOUSTICS AND VIBRATION RESEARCH (JAVR) ISSN: XXXX-XXXX VOL. 1. ISSUE 1. 2023. 41 – 52



Dynamic Characterisation of Thin Metal Plates using Piezoelectric Film Sensor

M.A.F. Ahmad^{1*}, M.Z. Nuawi¹, S. Abdullah¹ & M.F.M. Tahir¹

¹Department of Mechanical & Manufacturing Engineering, Faculty of Engineering and Built Environment, Universiti Kebangsaan Malaysia, 43600 Bangi, Selangor, Malaysia.

*Corresponding email: muhamadariffadli@yahoo.com

ABSTRACT

Complete understanding and appreciation of dynamic properties, comprising of natural frequencies and mode shapes helps in designing a structural system, to ensure safety and reliability. They could be determined via modal analysis. This study highlighted the utilisation of a piezoelectric film sensor in experimental modal analysis to extract the relevant modal parameter from light metal structures. Square-shape metal plates, comprised of copper, galvanized steel, zink, brass and aluminium were used and configured in a free-free boundary condition, to ensure good modal estimation. Simple modal testing was arranged using impact hammer as impulse exciter and piezo-film as sensing element. A roving set of hammer tests as inputs was done on every structure which was marked by 9 grid points, whereas piezo-film was fixed on 3 locations to measure the outputs. Signals' input and output were combined to compute the frequency response function (FRF) and afterwards used to estimate and extract the modal parameter. On the other hand, theoretical values were derived by using Euler Bernoulli beam theory. As a result, the first 5 mode shapes with corresponding frequencies were determined and evaluated in both experiment and theory, and later on, compared for data's stability and validity. The outcome suggested satisfying experimental modal data which was in good agreement with theoretical', delivering an average of mean absolute percentage error (MAPE) of approximately 7.3%.

Article History

Received: 13/09/2022

Revised: 07/04/2023

Accepted: 17/04/2023

Published: 03/05/2023

Keywords: Experimental modal analysis; piezoelectric film sensor; Euler Bernoulli beam theory; free-free boundary condition; mode shape.

INTRODUCTION

In decades, modal analysis has become the main tool in defining, enhancing and optimising the dynamic attributes of engineering structures. It is a study of the structures' natural characteristics or dynamic properties, to describe them in terms of natural frequencies, mode shapes and damping factors. These characteristics could be extracted by performing either theoretical or experimental techniques.

The theoretical solution comprises of solving the partial differential equations, which are incorporated into normal differential equations of motion for a physical model having mass, stiffness and damping matrices. In addition, the theoretical scope could be enhanced by using a modern finite element analysis, allowing for the empowerment of any discrete linear dynamic structure. For instance, a simulation by applying finite element method (FEM) was done to evaluate, compare and optimize bridge structures' dynamic natural frequencies and properties [1]. Alternatively, the experimental part of the analysis can be performed with a technique known as modal testing. The exciter produces inputs while the sensor captures the response as outputs. The relationship between the vibration response and impulse from excitation is established as a function. It is generally known as frequency response function (FRF), which derive the modal model of a linear time-invariant vibratory system. The combination of all signals' responses and excitation collectively reflect the structural mutuality of the system; thus, the resonant frequencies and mode shapes could be graphically characterised and extracted descriptively [2].

Modal testing is usually performed by using a simple impact hammer or a shaker to excite the structure under test, while a sensor is used to acquire the response due to the excitation. A typical sensor mounted on an engineering structure for monitoring vibration response is often an integrated circuit accelerometer, which was still exploited for analysis, to date [3]. It is a lightweight transducer that provides high reliability and robustness in capturing vibration signals. However, having a small amount of mass could still affect the dynamical structure under study due to the roving mass effect, especially for thin and small samples [4]. The solution lies in mounting all the accelerometers on every location simultaneously to neutralise the effect, but this indirectly contributes to a higher operating cost. Another issue is the fixed sensitivity, meaning there are constraints on the range of data on which it can measure. Data clipping will occur if the actual signal is outside the limit, thereby give incorrect data [5]. The solution lies in using an accelerometer with better sensitivity, but eventually lead to higher expense. An alternative way to solve these problems is by having a low-cost, feather-like weight sensor, namely a piezoelectric film patch.

Piezoelectric materials exhibit a direct piezoelectricity effect which generates electric charges when mechanically deformed due to applied stress, thus, forcing the positive and negative charges to shift on the centre, subsequently stimulate an external electrical field. This is the reason why many sensors nowadays adapting the piezoelectric effect by having a small amount of piezoelectric material as a medium in their design framework. The fine examples are the microphone, accelerometer and ultrasonic transducer. Interestingly, piezoelectric materials could be used and fabricated as a standalone transducer, which ultimately leads to a low-cost, flexible and almost weightless piezoelectric film or patch sensor. They have been used extensively in a broad engineering research field and proven to be reliable. For example, Ramli et al. [6] applying the films to acquire the vibration responses of multiple impact forces to characterise Young modulus and Poisson's ratio on light structures. A slight error of less than 3% was found. In addition, they have also been used to measure the hybrid electric vehicle (HEV) engine's vibration signal and shown reliable results on diagnosing and predicting the stage of combustion [7]. Besides that, Ahmad et al. [8] investigated the potential of two types of films, namely composite and polymer, by extracting vibratory machining signals in tool wear monitoring. Both prevailed, with the former shown better result. On the other hand, Stamatellou & Kalfas [9] investigated the energy harvesting of the films positioned in turbulent flow with swirling air arrangement, in which they testified that a longer piezo-film increased the power output.

Piezo-film sensor has been previously used in modal testing, as asserted by Ramli et al. [10]. But the test was only limited to aluminium structures, meaning a broader type of structure is needed to test the reliability of the sensor. Besides, they primarily followed ASTM E1876 standard for structure's support which initiated a boundary condition where certain vibration modes were suppressed. Dynamic characteristics cannot be evaluated wholly, as some modes cannot be seen while others producing large errors due to misinterpretation. Hence, this paper will present the experimental modal analysis on various but light metal plate structures by employing piezoelectric film as a sensor. Five different sets of square-shape thin metals are chosen and placed in a free-free beam's boundary conditions, with each of them are mounted with a piezoelectric film patch. Simple modal testing is done using an impact hammer as an impulse exciter. Mode shapes with their corresponding natural frequencies are extracted using FRF estimation and later compare with theoretical values to verify the data and acquire the error.

METHODOLOGY

Experimental Set-Up and Procedure

Modal testing was done in a semi-anechoic chamber to eliminate external noise. A set of equipment was prepared for experiment and analysis, consisting of an impact hammer, piezoelectric film patch, data acquisition device, connection cables and a computer with LabVIEW and MATLAB software. Five square-shaped metal plates were used as a sample, comprising of copper, galvanized steel, zink, brass and aluminium. The same geometry size was selected across structures, with a value of 300 x 300 x 1.5 mm for length, width and thickness. Important materials used are summarised in Table 1 while the experimental work is shown in Figure 1.

Table 1. Material list

Tuote 1: Waterial list				
Apparatus	Type / Code / Description	Sensitivity / Specification		
Impact hammer	086C03 ICP® IMPACT	2.25 mV/N		
	HAMMER with steel insert tip	2.23 111 V/19		
Data Acquisition	NI-9234 module with cDAQ-	25 kS/s of sample rate		
Device	9171 Chassis	24-bit sample size's resolution		
Sensor	Piezoelectric film patch LDT1-	30 x 12 mm of active element		
	028K	(length x width)		
Sample	Copper, Galvanised steel, Zink,	300 x 300 x 1.5 mm		
	Brass and Aluminium	(length x width x thickness)		

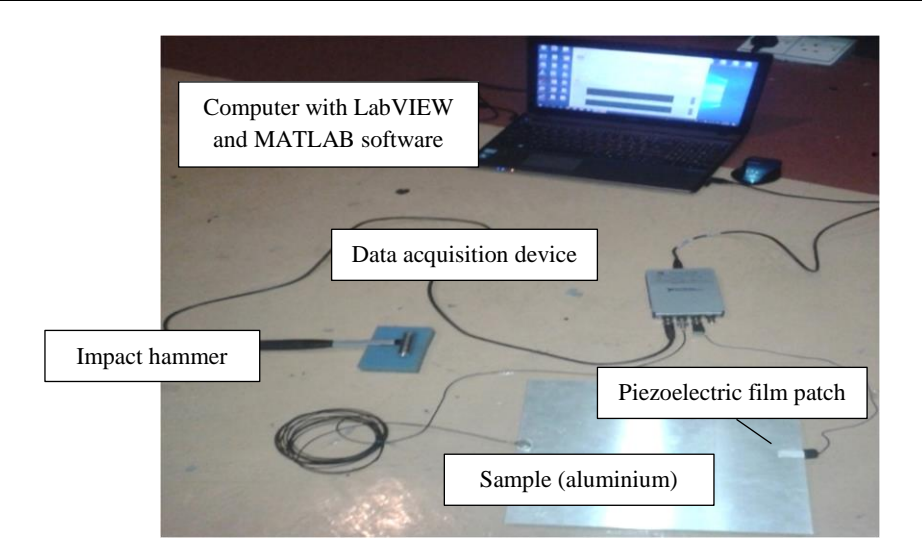


Figure 1. Modal testing

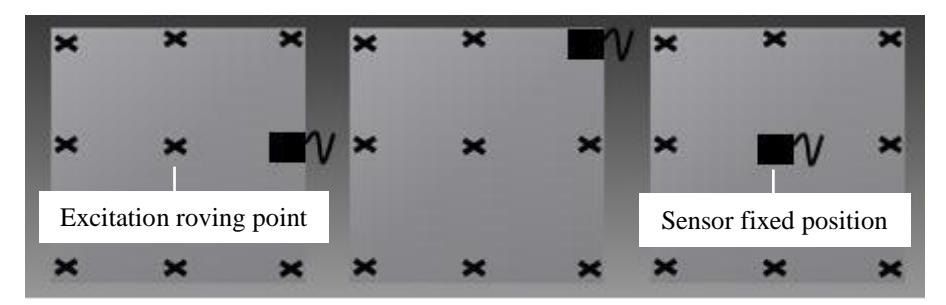


Figure 2. Impact excitation and sensor placement points

A sponge-like foam was mounted underneath the sample's structure, accumulating a whole back area to initiate a free-free boundary condition. The said configuration is preferred because it ensured a nearly perfect boundary condition and indirectly avoid uncertainties due to the support [11]. A total of 9 small grid points was divided equally on each of the plates, where a roving of hammer test on the points' location was carried out on all of the structure's marked points. The test initiated SISO testing condition, involving a single excitation point as input and a single vibration response as output for a particular measurement. Impact hammer was used to excite the structure on every point while piezoelectric film patch captured the vibration response. Three positions were fixed for the piezoelectric film sensor on every plate. For each of the sensor's placement, a roving set of impact tests was done and recorded together with corresponding vibration responses, therefore, resulting in 3 sets of data. The recording session was done using LabVIEW software environment. The sensor's position and impact's excitation points were illustrated in Figure 2.

Each roving set of impact's force inputs were combined with piezoelectric film's vibration response outputs to derive a single FRF. Thus, these combinations granted 3 FRFs corresponding to the sensor's fixed locations for each structure. FRF was computed using MATLAB programming software. Figure 3 displays the complete procedure for FRF extraction for impact testing.

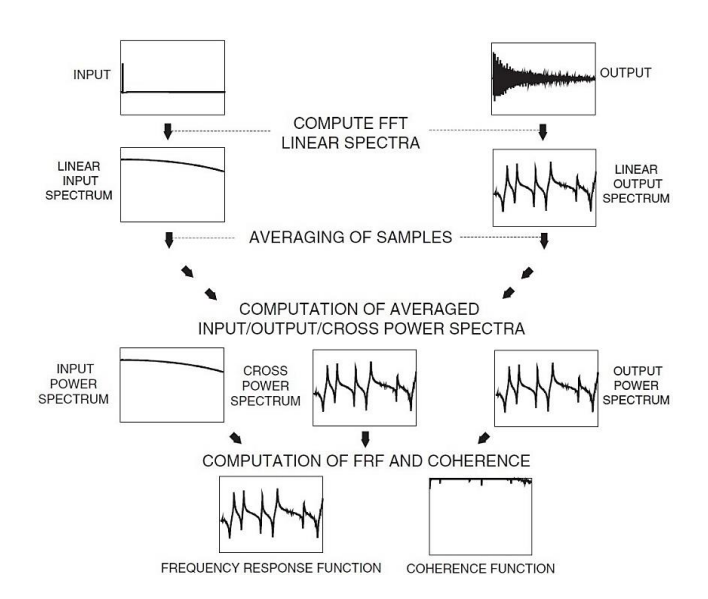


Figure 3. The overall process of FRF extraction from impact testing

THEORETICAL MODAL ANALYSIS

A simple Euler Bernoulli beam theory was followed instead of Timoshenko for the theoretical calculation of structure's dynamic characteristics. This is mainly because the length to thickness ratio of structures was fairly large, thus rotation and transverse shear strain have no significant effect on the dynamical behaviour of the beam [12]. In this case, rotary inertia and shear deformation were of minor importance, thereby, neglected. The absence of transverse load yielded the beam's equation of motion for free vibration, as presented by Equation 1.

$$EI\frac{d^4w}{dx^4} + \rho A\frac{d^2w}{dt^2} = 0 {1}$$

Where E is the young's modulus, I is the second moment of area of beam's cross-section, ρ is density and A is beam's cross-section. The general equation for free vibration by solving Equation 1 is therefore derived in Equation 2 [13].

$$w_n(x) = C_1(\cosh\beta_n x) + C_2(\cos\beta_n x) + C_3(\sinh\beta_n x) + C_4(\sin\beta_n x) \tag{2}$$

Where w_n are the natural frequencies of the beam. The constant values of C_1 , C_2 , C_3 and C_4 were defined from the beam's boundary conditions. Displacement solution is a mode and the shape of the curve is the mode shape. In the case of a free-free beam where there was no support configuration, bending moment and shear force was zero at both ends, and presented in Equation 3.

$$\frac{d^2w}{dx^2} = 0, \frac{d^3w}{dx^3} = 0 \qquad \text{for } x = 0, \ x = L$$
 (3)

By applying these conditions, non-trivial solutions are found to exist only if Equation 4 below is satisfied.

$$cosh\beta Lcos\beta L - 1 = 0 \tag{4}$$

This nonlinear equation has infinite solutions and could be solved numerically for every mode. The natural frequency of beam, ω_n with each mode is formulated as in Equation 5.

$$\omega_n = (\beta_n L)^2 \sqrt{\frac{EI}{\rho A L^4}} \tag{5}$$

The mode shape can therefore be illustrated as in Equation 6.

$$w_n = \left[\sinh\beta_n x + \sin\beta_n x\right] + \left[\cosh\beta_n x + \cos\beta_n x\right] \frac{\sin\beta_n x + \sinh\beta_n x}{\cos\beta_n x + \cosh\beta_n x} \tag{6}$$

To validate the accuracy of the experimental result, extracted natural frequencies with modes from FRF were compared with theoretical values by using a common indicator metric, namely mean absolute percentage error (MAPE). The absolute error is quantified as in Equation 7.

$$\Delta E = \left| x_{exp} - x_{th} \right| \tag{7}$$

 x_{exp} and x_{th} are experimental and theoretical values. The accuracy between predicted and observed values is measured as in Equation 8.

$$MAPE = \frac{100}{n} \sum_{i}^{n} \frac{\Delta E}{x_{th}}$$
 (8)

The whole methodology is summarized as in Figure 4.

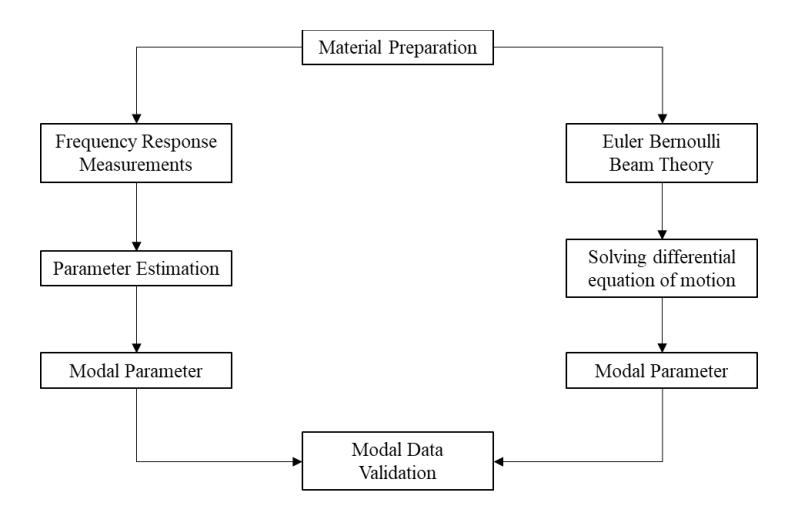


Figure 4. Flowchart of modal analysis process

RESULTS AND DISCUSSION

Impulse Force and Vibration Response

Two types of signals were identified from the experimental modal test extraction; input impact forces and output vibration responses. The input and output signals from copper plate structure are taken as an example and illustrated in Figure 5.

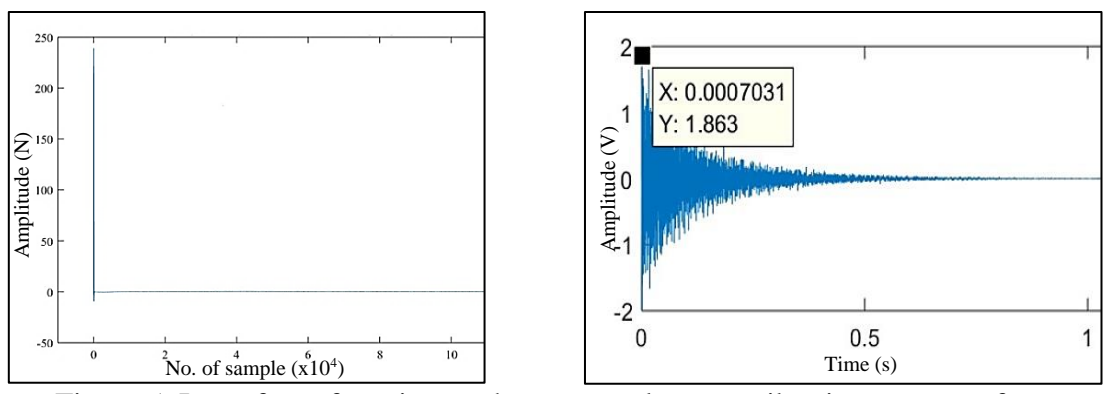


Figure 5. Input force from impact hammer and output vibration response from piezoelectric film patch

The figure is a time-domain graph of an impulse with a single impact force and a sensor's transient voltage response, which were applicable to all structures under study. The precaution was taken when performing roving hammer tests to avoid irrelevant responses due to double impact. The response indicated a good signal with free vibration characteristic, meaning the structure's body only vibrate due to the initial impact and was allowed to decay over time transiently without external force.

Frequency Response Function

Both input and output signals were subjected to FFT computation to produce output power spectrums and subsequently derived the FRF and coherence function for modal estimation. Each structure yielded 3 FRF graphs corresponding to sensor's fixed location, as seen in Figure 5 until Figure 9.

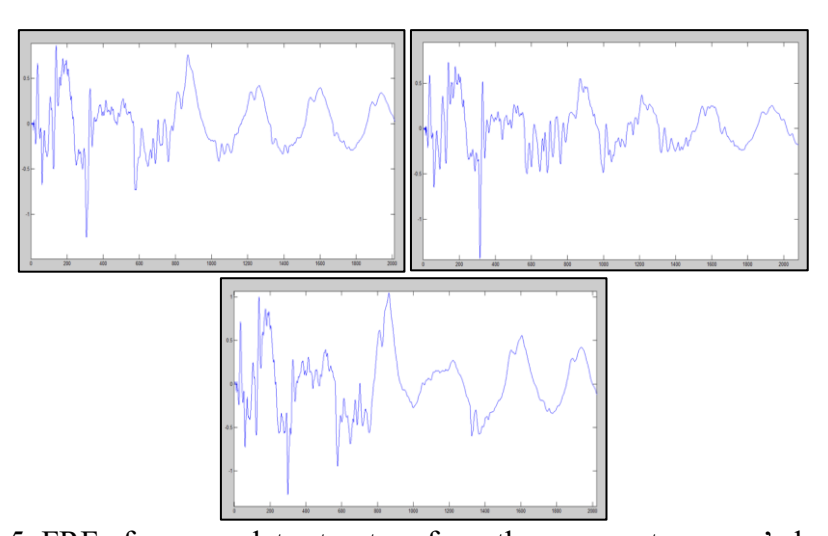


Figure 5. FRF of copper plate structure from three separate sensor's locations

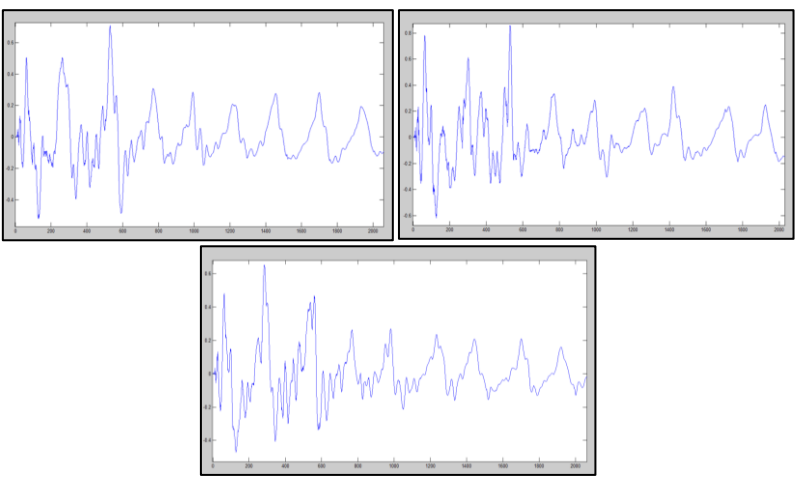


Figure 6. FRFs of galvanized steel plate structure from three separate sensor's locations

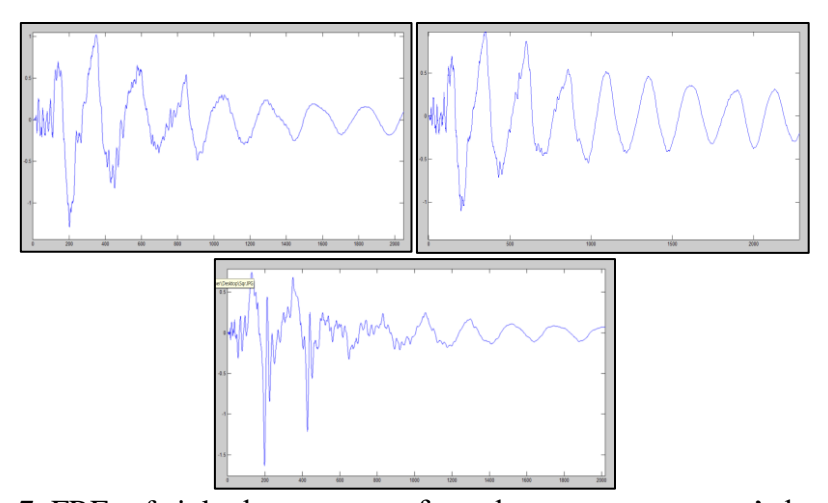


Figure 7. FRFs of zink plate structure from three separate sensor's locations

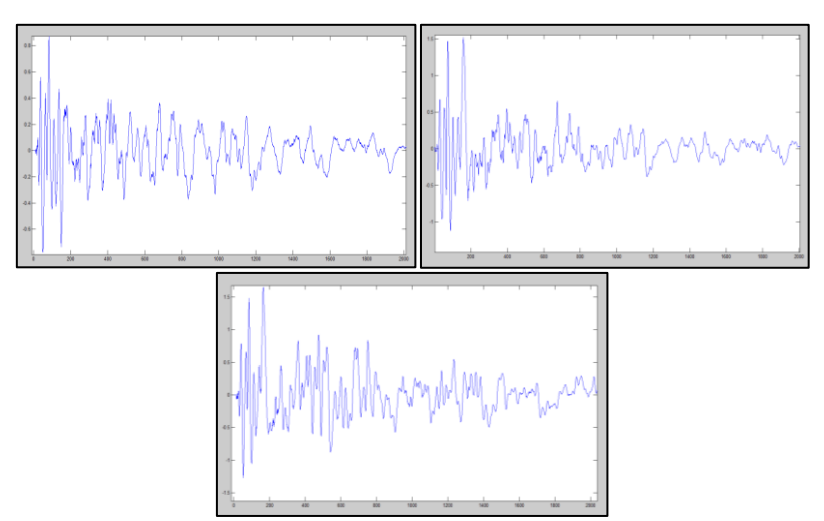


Figure 8. FRFs of brass plate structure from three separate sensor's locations

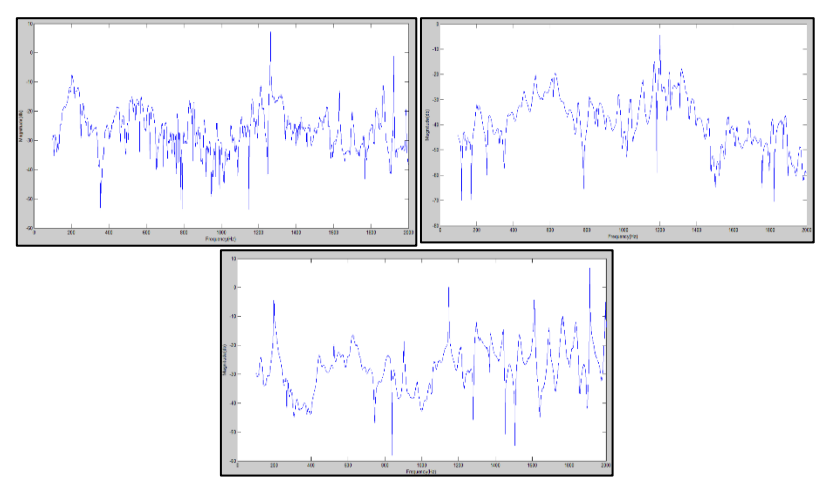


Figure 9. FRFs of aluminium plate structure from three separate sensor's locations

Modal Parameter Estimation

The first 5 mode shapes were observed and estimated by comparing and overlapping all FRFs for each structure. The purpose was to find and extract the peaks related to the natural frequencies with respect to vibration modes. As a result, natural frequencies for each structure, separated by their mode shape numbers are tabulated in Table 2.

Table 2. Modal parameters from FRF

Material	Natural Frequency (Hz)					
Material	1	2	3	4	5	
Copper	65.73	151.89	328.05	527.37	859.12	
Galvanised Steel	74.38	258.51	511.27	770.82	1008.56	
Zink	67.45	150.16	350.87	591.54	854.36	
Brass	66.96	161.27	352.22	480.03	761.97	
Aluminium	89.29	202.67	520.18	828.33	1143.42	

Later, similar to experimental modal parameters, 5 mode shapes were also derived from theoretical solution, by applying Equation 5 for natural frequency derivation and Equation 6 for mode shape evaluation. The first five-mode shape graph based on Euler Bernoulli beam theory is depicted in Figure 10 while the extracted theoretical modal data are represented in Table 3.

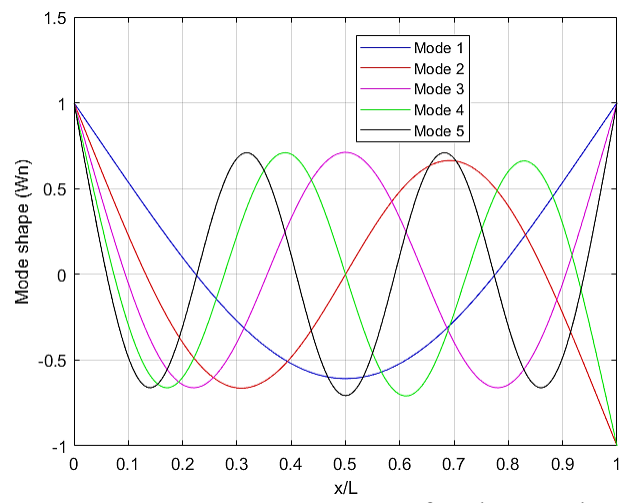


Figure 10. The first 5 modes of a vibrating free-free beam's boundary condition

rable 3. Wodai parameters from theoretical solution						
Material	Natural Frequency (Hz)					
Material	1	2	3	4	5	
Copper	62.05	171.03	335.30	554.26	827.97	
Galvanised Steel	86.75	239.13	468.80	774.94	1157.63	
Zink	63.16	174.10	341.31	564.21	842.83	

176.35 238.56 345.72

467.68

571.50

773.09

853.72

1154.86

63.98

86.54

Table 3. Modal parameters from theoretical solution

Modal Data Validation

Brass

Aluminium

Higher mode shapes directly contribute to higher natural frequencies. A correlation is usually done to compare the consistency of the experimental mode shapes and natural frequencies with numerical methods [14]. For simplicity, a correlation between natural frequencies and mode shape numbers were done using linear regression to verify the stability of the obtained modal data. The result is shown in Figure 11.

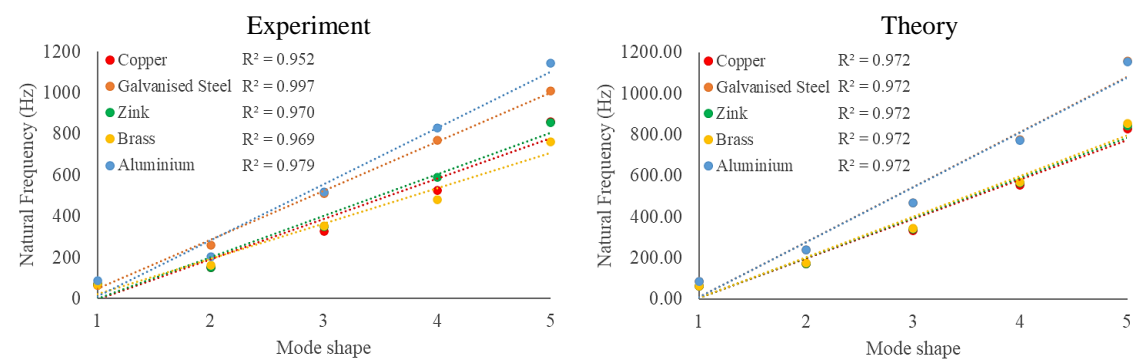


Figure 11. Correlation between natural frequency and mode shape from experiment and theoretical derivation

Curve fitting was applied to obtain a correlation of determination, R². Theoretical modal data shows the same R² across all structures with a value of 0.972, due to the same mathematical concept and derivation used. R² close to 1 proved that the theoretical part was valid. Meanwhile, the experimental part demonstrated the same graph pattern where a higher frequency was produced with a higher mode. R² values were different over each structure though. The lowest one being copper with 0.952 and the highest being galvanized steel with 0.997. The others with ascending order are brass, zink and aluminium, with the values of 0.969, 0.970 and 0.979, respectively. Even so, all structures' experimental modal data were good, as they follow the theoretical pattern, with R² surpassing the confidence level of 0.95.

To facilitate the validation of experimental modal data, they were compared with theoretical values and the result is tabulated in Table 4. A higher value of MAPE indicated a higher error between experiment and theory. The highest one being galvanized steel with 9.0% error, while the lowest is copper with 5.6%. The others are zink, aluminium and brass with 5.9, 7.5 and 8.4% of error, in ascending order. All structures established satisfying results with an error's nominal percentage of less than 10%. The average of

MAPE was calculated and overall, the final verdict showed that the results were all well within the reasonable margin, with approximately 7.3% error.

Table 4. Mean Absolute Percentage Error

		010			"8" = 11 11		
Material	ΔE				$\sum \Delta E$	MAPE	
	1	2	3	4	5	$\sum^{\Delta E}$	WAFE
Copper	0.059	0.112	0.022	0.049	0.038	0.279	5.6%
Galvanised	0.143	0.081	0.091	0.005	0.129	0.448	9.0%
Steel							
Zink	0.068	0.138	0.028	0.048	0.014	0.296	5.9%
Brass	0.047	0.086	0.019	0.160	0.107	0.418	8.4%
Aluminium	0.032	0.150	0.112	0.071	0.010	0.376	7.5%
Average Error							7.3%

CONCLUSIONS

Experimental modal analysis with free-free boundary conditions of various metal plates has been determined by utilising a piezoelectric film sensor. The first 5 mode shapes were clarified and compared with Euler Bernoulli beam's theoretical values for verifying modal data's stability and accuracy. The overall dynamical characteristic performance across all structures was measured using MAPE which yielded minimal error with an average of 7.3%. Henceforth, the reliability of the piezoelectric film sensor on estimating the modal parameter experimentally was proven in various metal plates with unconstrained bodies.

ACKNOWLEDGEMENTS

The authors would like to thank Universiti Kebangsaan Malaysia (UKM) and Ministry of Higher Education of Malaysia (KPT) for supporting this research study, by providing the laboratory facilities, necessary equipment and financial support through FRGS/1/2019/TK07/UKM/02/5 research grant.

REFERENCES

- [1] A. F. Naser, "Dynamic Analytical Modeling of Horizontal Outline Turn of T-Girder Simply Supported Bridge," Jurnal Kejuruteraan, vol. 33, no. 2, pp. 353-364, 2021.
- [2] P. Avitabile, Modal testing: a practitioner's guide, John Wiley & Sons, 2017.
- [3] M. Kalybek, M. Bocian, and N. Nikitas, "Performance of Optical Structural Vibration Monitoring Systems in Experimental Modal Analysis," Sensors, vol. 21, no. 4, pp. 1239, 2021.
- [4] M. Dumont, A. Cook, and N. Kinsley, "Acceleration measurement optimization: mounting considerations and sensor mass effect," Topics in Modal Analysis & Testing, vol. 10, pp. 61-71, 2016.
- [5] J. R. Evans, R. M. Allen, A. I. Chung, E. S. Cochran, R. Guy, M. Hellweg, and J. F. Lawrence, "Performance of several low-cost accelerometers," Seismological Research Letters, vol. 85, no. 1, pp. 147-158, 2014.
- [6] M. I. Ramli, M. Z. Nuawi, M. R. M. Rasani, N. A. Ngatiman, M. F. Basar, and A. A. Ghani, "Analysis of Young Modulus and Poisson Ratio Using I-Kaz 4d Analysis

- Method Through Piezofilm Sensor," Journal of Physics: Conference Series, vol. 1529, no. 4, pp. 042025, 2020.
- [7] N. A. Ngatiman, and M. Z. Nuawi, "Pattern Recognition for HEV Engine Diagnostic using an Improved Statistical Analysis," Jurnal Kejuruteraan, vol. 31, no. 2, pp. 287-294, 2019.
- [8] M.A.F. Ahmad, M. Z. Nuawi, J. A. Ghani, S. Abdullah, and M. I. Ramli. "An investigation on tool wear monitoring using MFC and PVDF sensors via I-kazTM statistical signal analysis," Proceedings of Mechanical Engineering Research Day 2018, pp. 301-302, 2018.
- [9] A. M. Stamatellou, and A. I. Kalfas, "Experimental investigation of energy harvesting from swirling flows using a piezoelectric film transducer," Energy Conversion and Management, vol. 171, pp. 1405-1415, 2018.
- [10] M. I. Ramli, M. Z. Nuawi, S. Abdullah, M. R. M. Rasani, M. A. F. Ahmad, and K. K. Seng, "An investigation on light structure modal parameter by using experimental modal analysis method via piezofilm sensor," Jurnal Teknologi, vol. 79, no. 6, 2017.
- [11] L. Barboni, G. R. Gillich, C. P. Chioncel, C. O. Hamat, and I. C. Mituletu, "A method to precise determine the Young's modulus from dynamic measurements," IOP Conference Series: Materials Science and Engineering, vol. 416, no. 1, pp. 012063, 2018.
- [12] X. Zhang, D. Thompson, and X. Sheng, "Differences between Euler-Bernoulli and Timoshenko beam formulations for calculating the effects of moving loads on a periodically supported beam," Journal of Sound and Vibration, vol. 481, pp. 115432, 2020.
- [13] J. K. Sharma, "Theoretical and experimental modal analysis of beam," Engineering Vibration, Communication and Information Processing, pp. 177-186, 2019.
- [14] I. Nadkarni, R. Bhardwaj, S. Ninan, and S. P. Chippa, "Experimental modal parameter identification and validation of cantilever beam," Materials Today: Proceedings, vol. 38, pp. 319-324, 2021.